

Periodic Orbits and Binary Collisions in the Classical Coulomb Three-Body Problem

Mitsusada M. Sano

*Graduate School of Human and Environmental Studies,
Kyoto University, Sakyo-ku, Kyoto, 606-8501, Japan*

Kiyotaka Tanikawa

National Astronomical Observatory of Japan, Mitaka, Tokyo, 181-8588, Japan

(Dated: March 8, 2022)

In the helium case of the classical Coulomb three-body problem in two dimensions with zero angular momentum, we develop a procedure to find periodic orbits applying two symbolic dynamics for one-dimensional and planar problems. A sequence of periodic orbits are predicted and are actually found numerically. The results obtained here will be a cornerstone for finding the remaining periodic orbits, which needed for semiclassical applications such as periodic orbit quantization.

PACS numbers: 05.45.Mt, 45.50.Jf, 34.10.+x

The microscopic three-body problem, for example, the helium atom, attracts both theoreticians and experimentalists because of rich structure of its spectrum. In particular, the excited states below the double ionization threshold ($E = 0$) show the most complicated spectral structure, and contain various information on electron-electron correlations. This spectral region is not only most interesting but also most difficult in both theoretical and experimental aspects. In investigating its spectrum, semiclassical methods inevitably face with chaotic nature of its classical dynamics [1]. In a theoretical aspect, for the collinear eZe configuration, the semiclassical periodic orbit quantization was carried out by using the celebrated Gutzwiller trace formula [2] within reasonable accuracy [3, 4]. However, such successes of semiclassical and classical approaches have been restricted to one-dimensional case, namely the collinear eZe and eeZ configurations and the Wannier ridge configuration [1, 3, 4, 5]. The helium atom in two dimensions remains as a challenging object.

Main difficulties are due to (1) the mixture of chaos and tori, (2) the high-dimensionality, and (3) the singular nature of its dynamics. To overcome these difficulties, one needs sophisticated mathematical tools. McGehee's blow-up transformation and the concept of the triple collision manifold [6] are important examples [7, 8, 9, 10, 11, 12, 13]. Thanks to these tools, the dynamics near triple collision and the structure of stable and unstable manifolds were elucidated to some extent. In fact, a quantum manifestation of triple collision was demonstrated [14, 15]. But we still know less about periodic orbits in two-dimensional dynamics, which are needed for semiclassical analysis.

Quite recently, one additional tool, i.e., the symbolic dynamics for the planar gravitational problem is developed [16]. In this method, binary collisions are naturally obtained as boundaries of different symbol sequences. We already have one-dimensional symbolic dynamics [8]. Then, we can systematically search periodic orbits in

the dynamics with zero initial velocities (DZIV) using one-dimensional and two-dimensional symbolic dynamics. We do this in the present report.

As is known in [10], the initial condition space of the DZIV is bounded by the collinear initial conditions (see below). First, using the two-dimensional symbolic dynamics, we numerically confirm the existence of curves of initial conditions of orbits exhibiting binary collisions. We call these the binary-collision curves (BCCs). Next, we go back to symbolic dynamics for the collinear problem and obtain symbol sequences of triple collision orbits. As predicted in [10], a sequence of BCCs is shown to have two end-points on $\alpha = \pi$. In other words, these BCCs can be uniquely specified by the end-points. Then, we informally consider a one-dimensional symbolic dynamics along BCCs and obtain self-retracing periodic orbits along them. Our procedure (Fig. 3) will be justified by numerical integration (Fig. 4). Finally, we characterize periodic orbits with physical quantities.

Now we introduce the system considered. In the helium atom, two electrons are denoted by particles 1 and 2, and the nucleus is denoted by particle 3. Let \mathbf{r}_i be the position vector of the i th particle, and let $\mathbf{r}_{ij} = \mathbf{r}_i - \mathbf{r}_j$. We assume that the nucleus has infinite mass and that initial velocities of particles are zero, which implies that the problem is planar. Then, the Hamiltonian in the hyperspherical coordinates is given by

$$H = \frac{1}{2} \left(p_r^2 + \frac{4p_\chi^2}{r^2} + \frac{4p_\alpha^2}{r^2 \sin^2(\chi)} \right) - \frac{1}{r} \left(\frac{1}{\cos(\frac{\chi}{2})} + \frac{1}{\sin(\frac{\chi}{2})} - \frac{1}{Z[1 - \sin(\chi) \cos(\alpha)]^{1/2}} \right) \quad (1)$$

where $r = (r_1^2 + r_2^2)^{1/2}$ is the hyperradius with $r_1 = r \cos(\chi/2)$, $r_2 = r \sin(\chi/2)$, and $\chi = 2\arctan(r_2/r_1)$. $Z (= 2$ in this Letter) is the charge of the nucleus. Z appears in the denominator of the potential term because of the scaling of variables. α is the angle between the vectors \mathbf{r}_{13} and \mathbf{r}_{23} . The total energy is $E = H$.

Next we introduce symbolic dynamics [16]. Three particles from a triangle. The area of this triangle has the sign $\eta = \mathbf{e}_z \cdot (\mathbf{r}_{13} \times \mathbf{r}_{23}) / |\mathbf{r}_{13} \times \mathbf{r}_{23}|$. The length of the i th side of the triangle is $l_i = |\mathbf{r}_{jk}|$, where (i, j, k) is a cyclic permutation of $(1, 2, 3)$. If η changes its sign from plus to minus and $\max\{l_1, l_2, l_3\} = l_k$, then we assign a symbol k . If η changes its sign from minus to plus and $\max\{l_1, l_2, l_3\} = l_k$, then we assign a symbol $k+3$. Then we obtain a symbol sequence $\mathbf{s} = \bullet s_1 s_2 s_3 \dots$ for a given orbit with the symbol set $\mathbf{S} = \{1, 2, 3, 4, 5, 6\}$.

By scaling the system, we remove the dependence on r from the DZIV. Then the initial conditions are uniquely specified by $0 \leq \chi < \pi$ and $0 \leq \alpha < 2\pi$. Moreover, the quarter of the initial condition space $D_{1/4} = \{(\chi, \alpha) | 0 \leq \chi \leq \frac{\pi}{2}, 0 \leq \alpha \leq \pi\}$ suffices for our purpose owing to the symmetry of the problem. We integrate orbits starting at points in $D_{1/4}$, and assign a symbol sequence to each orbit following the procedure given in [16]. Then, $D_{1/4}$ is partitioned into regions of different symbol sequences. One example of partitions by symbol sequences up to symbol length 8 is shown in Fig. 1. The BCCs are clearly seen as the boundaries of the partitioned regions. This shows a big advance compared with [10]. In that work, BCCs were obtained point by point along them, so the task was rather time consuming. In addition, orbit integrations near $\alpha = \pi$ were difficult due to the closeness to triple collision. The present method basically avoids triple collision, so is accurate and fast.

The intersections of BCCs with $\alpha = \pi$ are the initial conditions for triple-collision orbits (TCOs). We call them the triple-collision points (TCPs). We attach, in Fig. 1, the orbits of some of the TCPs with symbol sequences 0, 210, 20, and 220 where '0' represents triple collision, '1' binary collision between particles 1 and 3, and '2' binary collision between particles 2 and 3. Hereafter the symbolic dynamics means the symbolic dynamics in the collinear eZe configuration.

We observe two groups of BCCs. One group, which we call the *first kind*, consists of the BCCs which start at $\alpha = \pi$ and end at $\alpha = \pi$. We denote a BCC of this group by a lobe from its shape, and express it as $w_m 0 - w_n 0$ using the symbol sequences $w_m 0$ and $w_n 0$ of the left and right end points where w_k is a word of length k . The other, which we call the *second kind*, consists of the BCCs which start at $\alpha = \pi$ and end at $\alpha = 0$. There are other possibilities of the terminals of the BCCs. For our present purpose, we only consider periodic orbits on BCCs of the first kind. There exist an infinite number of TCPs on $\alpha = \pi$. Correspondingly, the number of lobes is infinite (see also Fig. 5 and [8]), which immediately implies that there exist infinitely many (unstable) POs on BCCs of the first kind, as we show later.

The appearance order of TCPs is illustrated in Fig. 2. If the symbol length is l , the total number of the TCPs appearing on $\alpha = \pi$ is 2^{l-1} where l denotes the *generation* of TCPs. The successive generations of TCPs are

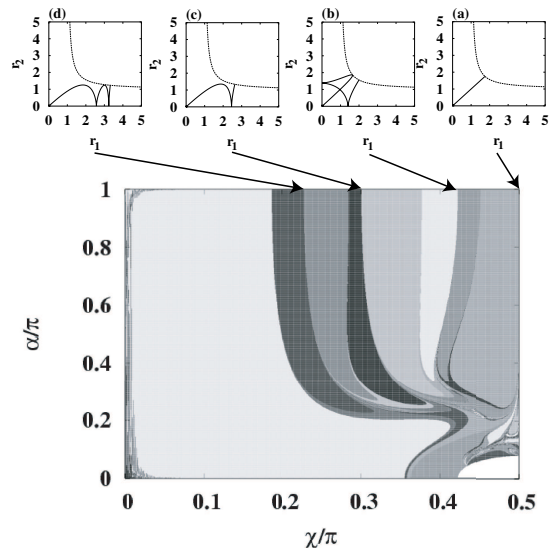


FIG. 1: Partition in $D_{1/4}$ and triple-collision points in the collinear eZe configuration: The large figure represents the partition obtained from the symbol sequences of symbol length 8 in the symbolic dynamics for two-dimensional dynamics. The boundaries between the regions of the partition are binary-boundary curves. The small figures represent the triple-collision orbits in the collinear eZe configuration. (a) 0. (b) 210. (c) 20. (d) 220. The blank region at the lower-right corner is the forbidden region ($E > 0$).

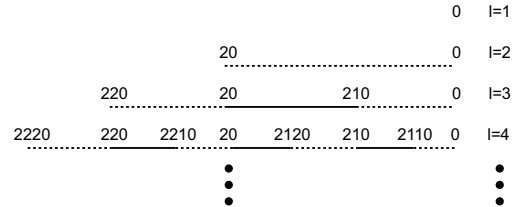


FIG. 2: Appearance of triple-collision points on the line $\alpha = \pi$: l is the symbol length in the symbolic dynamics for the collinear eZe dynamics. The symbol sequences of triple-collision orbits on $\alpha = \pi$ are represented in the symbolic dynamics of the collinear eZe case. The solid (resp. dotted) line represents the lobe corresponding to 2-3 (resp. 1-3) collision.

connected by the following rule: In the $(l+1)$ th generation, new TCPs are added in between the already existing TCPs in the l th generation. Let w be a word of length $l-1$, and $w0$ be a symbol sequence of a TCP which already exists in the l th generation. Then, $w10$ appears to the immediate right of $w0$, while $w20$ appears to the immediate left of $w0$. (The former rule does not apply for $l=1$.) Any orbit in BCCs with this new $w10$ or $w20$ at the right (resp. left) end experiences a 2-3 (resp. 1-3) collision.

Here we give an intuitive proof of the existence of a PO on each BCC of the first kind (i.e., lobe). We introduce

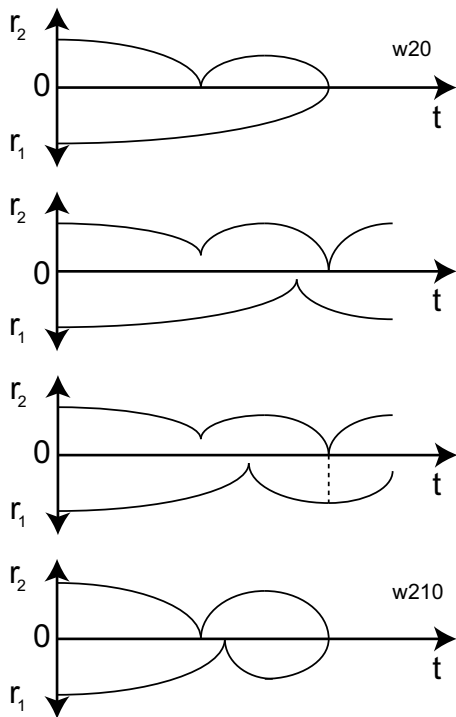


FIG. 3: Tails of orbits on the lobe $w20$ - $w210$

coordinate h ($0 \leq h \leq 1$) on the curve so that $h = 0$ at the left end and $h = 1$ at the right end. The orbit changes its topology when we move along the curve from $h = 0$ to $h = 1$ since the orbits at both ends have different histories of collisions. There are three types of lobes: (i) lobe $w20$ - $w0$ ($w \neq 2^k$, $k \geq 0$) or lobe $w0$ - $w10$; (ii) lobe $w0$ - $w'0$ where symbol lengths of w and w' differ by 2 or more; (iii) lobe $2^{k+1}0$ - 2^k0 ($k \geq 0$).

First consider case (i), i.e., the case of lobe $w20$ - $w210$. Let us move from $w20$ ($h = 0$) to $w210$ ($h = 1$). The relative position of the minimum of r_1 continuously changes as in Fig. 3. The triple collision at $h = 0$ becomes a 2-3 binary collision for $0 < h < 1$. As h increases, the next minimum of r_1 approaches the 2-3 binary collision from the right, and finally coincides with it at $h = 1$ resulting in triple collision. In this process, there exists a parameter value such that the 2-3 binary collision and the local maximum of r_1 take place at the same time (see the third panel of Fig. 3). At this moment, the angular momentum of electron 2 and the nucleus is zero with respect to their center of mass, which means that the angular momentum of electron 2 is zero, since the nucleus has infinite mass. This in turn means that the angular momentum of electron 1 is zero, which implies that electron 1 stands still at this moment. Then, both electrons retrace the path they tread, that is, a self-retracing PO is obtained. In the above proof, the persistence of the minima of r_1 and r_2 is crucial.

The proof for case (ii) may be similar to case (i). How-

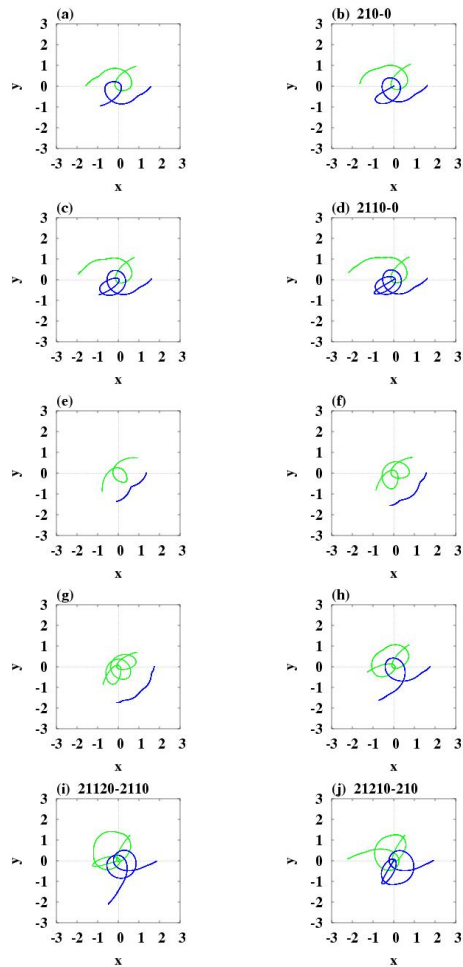


FIG. 4: (Color online) Periodic orbits (POs) found : The nucleus is fixed at the origin. For the POs with binary collisions, names of the lobe to which they belong are indicated. In the orbit integration, we set $E = -1$.

ever, there is a possibility that the orbit escapes, that is, one of electrons escapes to infinity. We skip this case, since we need a special care to treat the non-persistence of minima of r_1 and/or r_2 .

In case (iii), the situation is different from that of case (i). In this case, we can draw a similar orbital change as in Fig. 3. This time, however, the third minimum of r_2 disappears due to the escape of the orbit when the first minimum approaches the second minimum of r_2 . Then we do not have the simultaneous occurrence of the maximum of r_2 and the minimum of r_1 . Therefore, there is no POs on the $2^{k+1}0$ - 2^k0 lobes.

To obtain POs numerically, we look for the moment of zero velocities other than the initial moment. We actually carried out this procedure with many trials and errors. Then we find some POs using the improved Newton method.

We show example trajectories of POs in Fig. 4. We

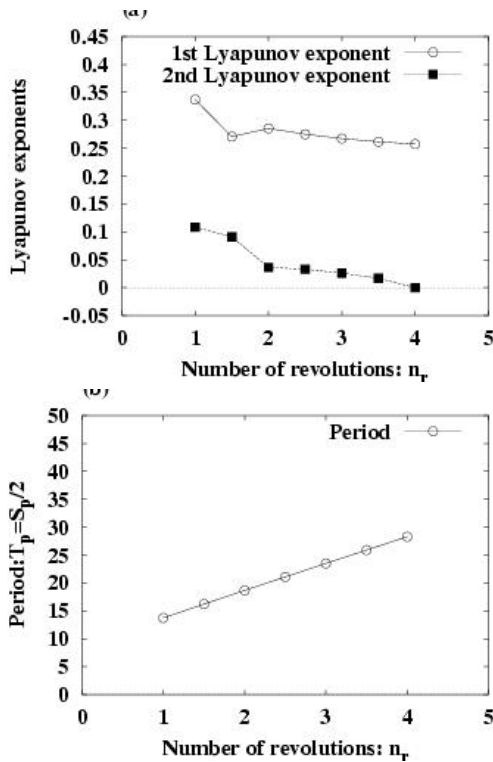


FIG. 5: The Lyapunov exponents and the period for a family of periodic orbits: (a) The Lyapunov exponents. (b) The period. n_r is the number of revolutions.

note one remarkable feature in these POs. One electron, by rapidly revolving round the nucleus, screens (or weakens) the Coulomb field which the other electron feels. During this phase, the other electron moves slowly. Two electrons alternate in one period between a rapid motion near the nucleus and a slow screened motion at a distance from the nucleus. Interestingly, the PO, which exhibits this alternation, is unstable. We found POs without binary collision through interpolation between two POs with binary collision. Some of stable frozen planetary orbits [17] are among them (see Figs. 4(e-g)).

Finally, we characterize POs as follows. In Figs. 4(a-d), it is clear that one electron revolves round the nucleus more than the other. Its number of revolutions up to the turn-back point (in the half period) is characterized by a half integer or an integer, say n_r . For Figs. 4(a-d), it is easily inferred that there exists a sequence of POs from $n_r = 1$ to $n_r = \infty$ (i.e., toward ionization). For these POs, the Lyapunov exponents and the period are numerically calculated (Fig. 5). It shows a remarkable regularity of the period, $T = S/2 = an_r + b$, where T is the period and S is the action.

Now taking the partial summation over n_r in the Gutzwiller periodic orbit sum $d_{\text{osc}}(E) = \sum_p A_p e^{\frac{i}{\hbar} S_p}$ with a daring approximation, i.e., A_p is factored out and is replaced by the mean value \bar{A} , thanks to Poisson sum-

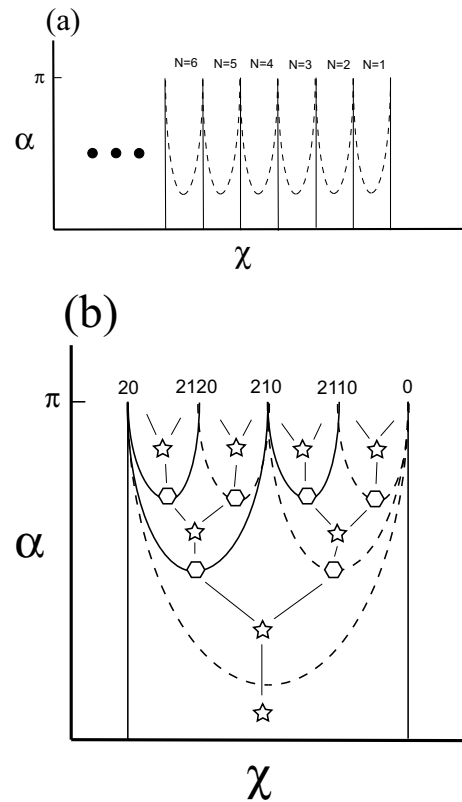


FIG. 6: Schematic pictures of binary-collision curves and periodic orbits (POs) in $D_{1/4}$: (a) Schematic picture of binary-collision curves (BCCs) of the first kind and the second kind. Solid (resp. dotted) lines represent the BCCs for 2-3 (resp. 1-3) collisions. There are infinite number of fundamental blocks. The fundamental block is numbered by N from the right hand side. (b) POs in the line $\alpha = \pi$: The triple collision orbits in the line $\alpha = \pi$ are indicated. The BCCs of the first kind are nested. The hexagon (resp. star) represents a position of a PO with (resp. without) binary collisions. The connected graph, which links the positions of the POs, is displayed.

mation formula, we obtain the Rydberg energy levels, $E_n = -\frac{C}{n^2}$ with constant C . This means that the regular structure found is important for the energy levels of the helium atom. The amplitude factor A_p may play a role of determining the quantum defects for the helium atom as observed in the collinear eZe case [4]. To complete this program to obtain the energy levels, we have to seek the geometrical structure of the whole (unstable) POs. The result of the present Letter is a hint to this problem.

In Fig. 6, a schematic disposition of BCCs and POs are illustrated. As shown in Fig. 6(a), there is a fundamental block between two BCCs of the second kind. The number of fundamental blocks is infinite (Fig. 6(a)). The fractal structure of BCCs and the tree structure of POs similar to a binary Cayley tree are expected to be topologically the same in every block (Fig. 6(b)) reflecting the fractal

distribution of TCPs on $\alpha = \pi$. We show in Fig. 6(b) the structure of the rightmost block. We find that there exists a PO on each lobe in Fig. 6(b), even on the lobe of case (ii). It is interesting to note that though POs are far from $\alpha = \pi$, they keep a kind of one-dimensionality along with other orbits in BCCs.

In conclusion, we have informally proved the existence of self-retracing POs with binary collisions, which form the backbone of the phase space, using the structure of BCCs and have indeed found such POs numerically. These findings would serve theoreticians with new stimuli, who would like to carry out the semiclassical treatment of the helium atom in two dimensions with zero angular momentum.

This work was supported by a Grant-in-Aid for Scientific Research (No.17740252) from the MEXT, Japan.

[1] G. Tanner, K. Richter, and J. -M. Rost, *Rev.Mod.Phys.* **72** 497 (2000).
 [2] M. C. Gutzwiller, *J.Math.Phys.* **12** 343 (1971).
 [3] G. S. Ezra K. Richter, G. Tanner, and D. Wintgen,

J.Phys.B **24** L413 (1991).
 [4] G. Tanner and D. Wintgen, *Phys.Rev.Lett.* **75** 2928 (1995).
 [5] K. Richter, G. Tanner, and D. Wintgen, *Phys.Rev.A* **48** 4182 (1993).
 [6] R. McGehee, *Invet.Math.*, **27**, 191 (1974).
 [7] Z. -Q. Bai, Y. Gu, and J. M. Yuan, *Physica D* **118** 17 (1998).
 [8] M. M. Sano, *J.Phys.A*, **37**, 803 (2004).
 [9] M. M. Sano, *Adv.Chem.Phys.*, **130**, Part A, 305 (2005).
 [10] M. M. Sano, *Phys.Rev.E*, **75**, 026203 (2007).
 [11] N. N. Choi, M. -H. Lee, and G. Tanner *Phys.Rev.Lett.*, **93**, 054302 (2004).
 [12] M. -H. Lee, G. Tanner, and N. N. Choi, *Phys.Rev.E*, **71**, 056208 (2005).
 [13] M. -H. Lee, N. N. Choi, and G. Tanner, *Phys.Rev.E*, **72**, 066215 (2005).
 [14] C. W. Byun, N. N. Choi, M. -H. Lee, and G. Tanner, *Phys.Rev.Lett.*, **98**, 113001 (2007).
 [15] G. Tanner, N. N. Choi, M. -H. Lee, A. Czasch and R. Dörner, *J.Phys.B*, **40**, F157 (2007).
 [16] K. Tanikawa and S. Mikkola, e-print arXiv:0802.2465 (2008).
 [17] K. Richter and D. Wintgen, *Phys.Rev.Lett.* **65** 1965 (1990).